Recent Advances on Reduced Order Modelling for viscous and thermal flows in parametrized settings: focus on stability and bifurcations

Workshop on Model Order Reduction of Transport-dominated Phenomena
Berlin-Brandenburg Academy of Sciences
Berlin, Germany
May 19-20, 2015

Gianluigi Rozza

SISSA, International School for Advanced Studies, Trieste, Italy, Mathematics area,
Joint work with **Giuseppe Pitton** (SISSA) and **Annalisa Quaini** (University of Houston)

Outline

MOTIVATION

- At the state of the art, Reduced Order Modelling (ROM) in CFD is finding a good growth in methodological and computational developments (RB, POD, PGD), and several real applications;
- Stability of the reduced approximation, error bounds, sampling techniques have been studied and improved in the past few years;
- The current goal is to increase Reynolds number and to have a deeper knowledge of complex Fluid Dynamics phenomena such as flow bifurcations and stability (also in cardiovascular flows) through reduced eigenproblems.

Preliminaries: what is a bifurcation in a system?

Many physical systems show a sudden change in behaviour as one or more control parameters are smoothly varied.

First example: Rayleigh-Benard convection problem (X-roll(s)-flow)

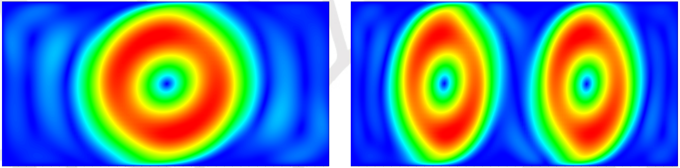

This kind of behaviour is studied in bifurcation theory [Ambrosetti, Prodi].
Focus:

- → Nonlinearities;
- → Non-uniqueness of the solution.

This will be used as model problem (other cases: buckling of a structure and critical loads, "squeal" in automotive disk brakes: noise after resonance frequency [V.Mehrmann]).
Reduced basis method is used in nonlinear structural mechanics, POD is born in CFD (turbulence), HPC was a dream [Noor et al., 1981], [Peterson, 1989].

Why do some problems bifurcate?

We consider problems dependent on a parameter $\lambda \in \mathbb{R}^n$.

Abstract setting

Given $\lambda \in \mathbb{R}^n$, find $u \in X$ such that

$$F(\lambda, u) = 0$$
$$F : \mathbb{R}^n \times X \to Y$$

With X, Y Banach spaces.

Typical case: $Y = X$, $F(\lambda, u) = \lambda \mathcal{L} u + \mathcal{N}(u)$. Often the parameter affects only the linear part $\mathcal{L}$ of the operator.

The nonlinearity $\mathcal{N}(u)$ can produce a loss of uniqueness for u, and introduce multiple branches of solutions, at least for some ranges of the parameters.

When multiple solutions start branching from a known solution, we say that a bifurcation point has appeared.

Focus: computational reduction strategies for viscous and thermal flows

Goal

To achieve the *accuracy* and *reliability* of a high fidelity approximation but at a greatly *reduced cost* of a *low order model*.

Real-time or many-query computational settings related with bifurcation problems:

- → evaluation of flow stability under perturbations;
- → identification of steady bifurcation points;
- → identification of Hopf bifurcation points;
- → many possible applications: tribology, micro-fluid dynamics, aerodynamics, industrial flows, haemodynamics, . . .

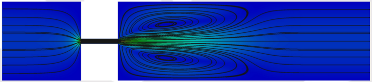

before bifurcation

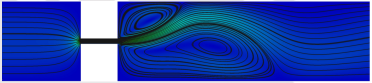

after steady bifurcation

Leading motivation (with Annalisa Quaini, University of Houston)

Mitral valve Regurgitation (MR) is a valvular heart disease associated with the abnormal leaking of blood from the left ventricle into the left atrium of the heart.

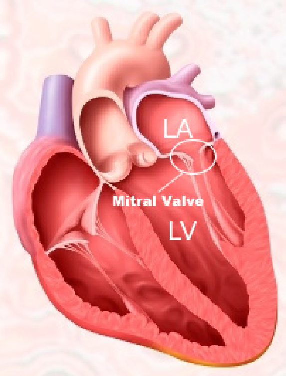

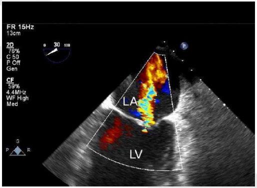

central jet

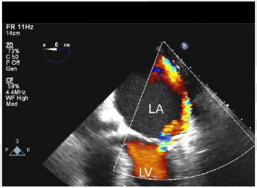

eccentric jet

Acknowledgments: S. Canic, R. Glowinski, S. Little MD, S. Igo MD, W. Zoghbi MD, Dr. C. Hartley (U. of Houston and their medical partners)

The Coanda effect in aerodynamics and cardiology

The COANDA EFFECT is the tendency of a fluid jet to be attracted to a nearby surface.
It is named after aerodynamics pioneer Henri Coanda (patent 1934).

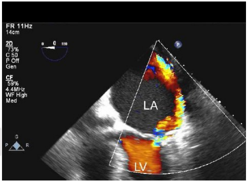

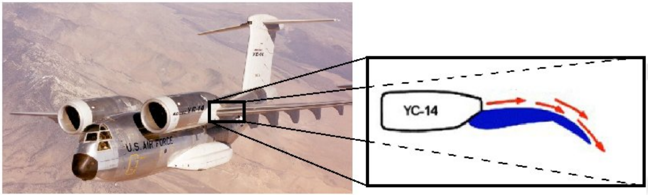

The YC-14 uses the Coanda effect to increase the lift for a short take off and landing.

One of the biggest challenges in the echocardiographic assessment of MR is the Coanda effect.

2D contraction-expansion channel

Let us simplify the geometry and understand under which conditions the Coanda effect is generated.

We consider the flow of an incompressible fluid in this 2D geometry

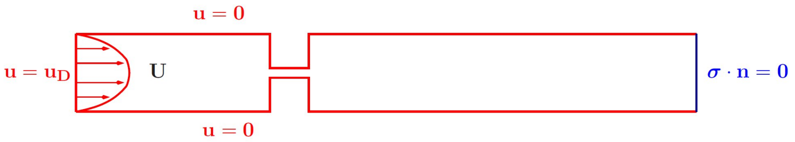

Re = 0.01

Re = 7.8

Re = 31.1

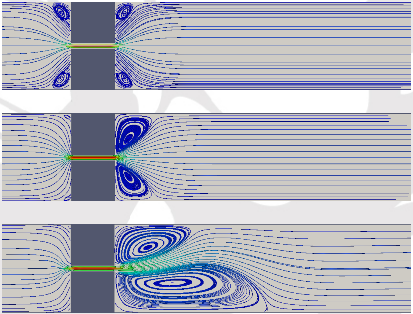

METHODOLOGY

Computational reduction: the idea

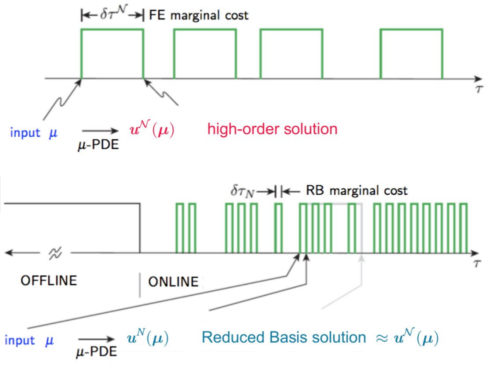

Acknowledgement: Anthony T. Patera (MIT) - `augustine.mit.edu`

Reduced Basis Methods: Construction

μ-PDE, weak formulation

$$\boldsymbol{u}(\boldsymbol{\mu}) \in \boldsymbol{V} : \qquad F_{\mathrm{NS}}(\boldsymbol{\mu}; \boldsymbol{u}(\boldsymbol{\mu}), \boldsymbol{v}) = 0 \qquad \forall \boldsymbol{v} \in \boldsymbol{V}$$

Truth approximation (FEM, SEM, ...)

$$\boldsymbol{u}^{\mathcal{N}}(\boldsymbol{\mu}) \in \boldsymbol{V}^{\mathcal{N}} : \qquad F_{\mathrm{NS}}(\boldsymbol{\mu}; \boldsymbol{u}^{\mathcal{N}}(\boldsymbol{\mu}), \boldsymbol{v}) = 0 \qquad \forall \boldsymbol{v} \in \boldsymbol{V}^{\mathcal{N}}$$

→ Truth Hypothesis: $\boldsymbol{u}^{\mathcal{N}}(\boldsymbol{\mu})$ "indistinguishable" from $\boldsymbol{u}(\boldsymbol{\mu})$.

→ RB Motivation: $\boldsymbol{\mu} \to \boldsymbol{u}^{\mathcal{N}}(\boldsymbol{\mu})$ too expensive and slow in many-query and real-time contexts.

Reduced Basis Methods: Construction

μ-PDE, weak formulation

$$\boldsymbol{u}(\boldsymbol{\mu}) \in \boldsymbol{V}: \qquad F_{\mathrm{NS}}(\boldsymbol{\mu}; \boldsymbol{u}(\boldsymbol{\mu}), \boldsymbol{v}) = 0 \qquad \forall \boldsymbol{v} \in \boldsymbol{V}$$

Truth approximation (FEM, SEM, ...)

$$\boldsymbol{u}^{\mathcal{N}}(\boldsymbol{\mu}) \in \boldsymbol{V}^{\mathcal{N}}: \qquad F_{\mathrm{NS}}(\boldsymbol{\mu}; \boldsymbol{u}^{\mathcal{N}}(\boldsymbol{\mu}), \boldsymbol{v}) = 0 \qquad \forall \boldsymbol{v} \in \boldsymbol{V}^{\mathcal{N}}$$

Sampling (Greedy, CVT, ...)
Space construction
(Hierarchical Lagrange basis)
OFFLINE

$$S^N = \{\boldsymbol{\mu}^i, i = 1, \ldots, N\}$$
$$\boldsymbol{V}^N = \mathrm{span}\{\boldsymbol{u}^{\mathcal{N}}(\boldsymbol{\mu}^i), i = 1, \ldots, N\}$$

Reduced Basis Methods: Construction

μ-PDE, weak formulation

$$\boldsymbol{u}(\boldsymbol{\mu}) \in \boldsymbol{V}: \qquad F_{\mathrm{NS}}(\boldsymbol{\mu}; \boldsymbol{u}(\boldsymbol{\mu}), \boldsymbol{v}) = 0 \qquad \forall \boldsymbol{v} \in \boldsymbol{V}$$

Truth approximation (FEM, SEM, ...)

$$\boldsymbol{u}^{\mathcal{N}}(\boldsymbol{\mu}) \in \boldsymbol{V}^{\mathcal{N}}: \qquad F_{\mathrm{NS}}(\boldsymbol{\mu}; \boldsymbol{u}^{\mathcal{N}}(\boldsymbol{\mu}), \boldsymbol{v}) = 0 \qquad \forall \boldsymbol{v} \in \boldsymbol{V}^{\mathcal{N}}$$

Sampling (Greedy, CVT, ...)
Space construction
(Hierarchical Lagrange basis)
OFFLINE

$$S^N = \{\boldsymbol{\mu}^i, i = 1, \dots, N\}$$
$$\boldsymbol{V}^N = \mathrm{span}\{\boldsymbol{u}^{\mathcal{N}}(\boldsymbol{\mu}^i), i = 1, \dots, N\}$$

Reduced basis (RB) approximation:
Galerkin projection

$$\boldsymbol{u}^N(\boldsymbol{\mu}) \in \boldsymbol{V}^N: \qquad F_{\mathrm{NS}}(\boldsymbol{\mu}; \boldsymbol{u}^N(\boldsymbol{\mu}), \boldsymbol{v}) = 0 \qquad \forall \boldsymbol{v} \in \boldsymbol{V}^N$$

ONLINE

$$N \equiv \dim \boldsymbol{V}^N \ll \mathcal{N} \equiv \dim \boldsymbol{V}^{\mathcal{N}}$$

Review: [Rozza et al., 2008]

FORMULATION OF THE PROBLEM

Parametrized weak formulation of the Navier-Stokes equations

For a given $\boldsymbol{\mu} \in \mathcal{D}$, find $(\boldsymbol{u}, p) \in \boldsymbol{V} \times Q$ such that

$$\begin{cases} m(\mu; \boldsymbol{u}, \boldsymbol{v}) + c(\boldsymbol{\mu}; \boldsymbol{u}, \boldsymbol{u}, \boldsymbol{v}) + a(\boldsymbol{\mu}; \boldsymbol{u}, \boldsymbol{v}) + b(\boldsymbol{\mu}; \boldsymbol{v}, p) = f(\boldsymbol{\mu}; \boldsymbol{v}) & \forall \boldsymbol{v} \in \boldsymbol{V} \\ b(\boldsymbol{\mu}; \boldsymbol{u}, q) = 0 & \forall q \in Q. \end{cases}$$

where

$$a(\boldsymbol{\mu}; \boldsymbol{u}, \boldsymbol{v}) = \int_{\overline{\Omega}(\boldsymbol{\mu})} \nabla \boldsymbol{u} : \nabla \boldsymbol{v} \, \mathrm{d}\overline{\boldsymbol{x}} \qquad b(\boldsymbol{v}, q) = \int_{\overline{\Omega}(\boldsymbol{\mu})} q \, \mathrm{div}\, \boldsymbol{v} \, \mathrm{d}\overline{\boldsymbol{x}}$$

$$m(\boldsymbol{\mu}; \boldsymbol{u}, \boldsymbol{v}) = \int_{\overline{\Omega}(\boldsymbol{\mu})} \boldsymbol{v} \cdot \frac{\partial \boldsymbol{u}}{\partial t} \, \mathrm{d}\overline{\boldsymbol{x}} \qquad c(\boldsymbol{\mu}; \boldsymbol{u}, \boldsymbol{w}, \boldsymbol{v}) = \int_{\overline{\Omega}(\boldsymbol{\mu})} \boldsymbol{v} \cdot (\boldsymbol{u} \cdot \nabla \boldsymbol{w}) \, \mathrm{d}\overline{\boldsymbol{x}}$$

$$f(\boldsymbol{\mu}; \boldsymbol{v}) = \int_{\overline{\Omega}(\boldsymbol{\mu})} \mathrm{Gr}\, \vartheta \boldsymbol{\jmath} \cdot \boldsymbol{v} \, \mathrm{d}\overline{\boldsymbol{x}}$$

Grashof number $\mathrm{Gr} = \frac{g\beta\Delta\vartheta H^4}{\nu^2 L}$.

The parametrized (original) domain $\overline{\Omega}(\boldsymbol{\mu})$ is the image of a fixed (reference) domain Ω through a parametric map $\mathcal{T}^{\mathrm{aff}}(\boldsymbol{x}, \boldsymbol{\mu}) : \Omega \to \overline{\Omega}(\boldsymbol{\mu})$.

A very important assumption is the *affine parameter dependence*, that allows to express the transformation as:

$$\overline{\boldsymbol{x}} = \mathcal{T}_i^{\mathrm{aff}}(\boldsymbol{x}, \mu) = C_i^{\mathrm{aff}} + \sum_{j=1}^{d} G_{ij}^{\mathrm{aff}}(\mu) x_j$$

for each subdomain $\overline{\Omega}_i(\mu)$. Using the standard change of variable theorems, the variational forms can be expressed on the reference domain:

$$\frac{\partial}{\partial \overline{x}_i} = \frac{\partial x_j}{\partial \overline{x}_i}\frac{\partial}{\partial x_j} = G_{ji}(\mu)\frac{\partial}{\partial x_j} \qquad \mathrm{d}\boldsymbol{x} = J^{\mathrm{aff}}(\mu)\,\mathrm{d}\overline{\boldsymbol{x}}$$

$$J^{\mathrm{aff}}(\mu) \equiv |\det(G^{\mathrm{aff}}(\mu))|$$

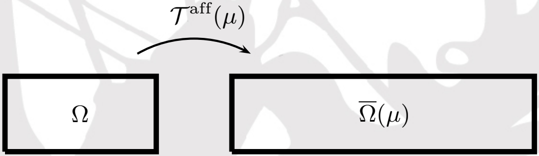

[several works on geometrical parametrization by FFD, RBF, TM,. . . , DD]

Reduced Basis Methods: smooth parametric dependency

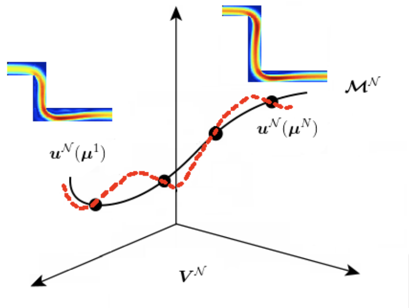

How to be rigorous, rapid and reliable?

i depends on the sampling procedure for parameter exploration;

ii exploits an Online/Offline stratagem based on the affinity assumption:

$$a(\boldsymbol{\mu}; \boldsymbol{v}; \boldsymbol{w}) = \sum_{q=1}^{Q_a} \Theta_a^q(\boldsymbol{\mu}) a^q(\boldsymbol{v}, \boldsymbol{w}), \cdots ;$$

iii relies on a posteriori error analysis.

Truth approximation (high-resolution)

High order approximation

Find $\boldsymbol{u}^{\mathcal{N}}(\boldsymbol{\mu}) \in \boldsymbol{V}^{\mathcal{N}}$ s. t.:

$$\begin{cases} m_h(\boldsymbol{\mu}; \boldsymbol{u}^{\mathcal{N}}(\boldsymbol{\mu}), \boldsymbol{v}) + c_h(\boldsymbol{\mu}; \boldsymbol{u}^{\mathcal{N}}(\boldsymbol{\mu}), \boldsymbol{u}^{\mathcal{N}}(\boldsymbol{\mu}), \boldsymbol{v}) + a_h(\boldsymbol{\mu}; \boldsymbol{u}^{\mathcal{N}}(\boldsymbol{\mu}), \boldsymbol{v}) & \\ \qquad + b_h(\boldsymbol{\mu}; \boldsymbol{v}, p^{\mathcal{N}}(\boldsymbol{\mu})) = f_h(\boldsymbol{\mu}; \boldsymbol{v}) & \forall \boldsymbol{v} \in \boldsymbol{V}^{\mathcal{N}} \\ b_h(\boldsymbol{\mu}; \boldsymbol{u}^{\mathcal{N}}(\boldsymbol{\mu}), q) = 0 & \forall q \in Q^{\mathcal{N}}. \end{cases}$$

We choose the Legendre Spectral Element Method, as implemented in the `Nek5000` open source software [Fischer et al., `http://nek5000.mcs.anl.gov`].

Main features:

- → spectral accuracy (if $\boldsymbol{u} \in C^{\infty}$):

$$\|\boldsymbol{u}(\boldsymbol{\mu}) - \boldsymbol{u}^{\mathcal{N}}(\boldsymbol{\mu})\|_{\boldsymbol{H}^1(\overline{\Omega}(\boldsymbol{\mu}))} \leq C\exp(-\gamma n), \quad \gamma > 0$$

- → very small dispersion error even for non-smooth solutions [Gottlieb and Orszag, 1977];
- → $\mathbb{P}_n - \mathbb{P}_n$ couple for velocity-pressure discretization, $n = 20$, 3rd order operator splitting in time [Tomboulides et al, 1997];

Reduced Basis Method: approximation stability and spaces

Reduced Basis approximation

Find $\boldsymbol{u}^N(\boldsymbol{\mu}) \in \boldsymbol{V}^N$ s. t.:

$$\begin{cases} m_h(\boldsymbol{\mu}; \boldsymbol{u}^N(\boldsymbol{\mu}), \boldsymbol{v}) + c_h(\boldsymbol{\mu}; \boldsymbol{u}^N(\boldsymbol{\mu}), \boldsymbol{u}^N(\boldsymbol{\mu}), \boldsymbol{v}) + a_h(\boldsymbol{\mu}; \boldsymbol{u}^N(\boldsymbol{\mu}), \boldsymbol{v}) & \\ \qquad + b_h(\boldsymbol{\mu}; \boldsymbol{v}, p^N(\boldsymbol{\mu})) = f_h(\boldsymbol{\mu}; \boldsymbol{v}) & \forall \boldsymbol{v} \in \boldsymbol{V}^N \\ b_h(\boldsymbol{\mu}; \boldsymbol{u}^N(\boldsymbol{\mu}), q) = 0 & \forall q \in Q^N. \end{cases}$$

Reduced basis spaces:

$$\boldsymbol{V}^N = \operatorname{span}\{\boldsymbol{\xi}^i \equiv \boldsymbol{u}^{\mathcal{N}}(\boldsymbol{\mu}^i), i = 1, \dots, N\} \qquad Q^N = \operatorname{span}\{\sigma_i \equiv p^{\mathcal{N}}(\boldsymbol{\mu}^i), i = 1, \dots, N\}$$

The reduced basis spaces must fulfill a parametrized LBB inf-sup condition

$$\inf_{q \in Q^N} \sup_{\boldsymbol{v} \in \boldsymbol{V}^N} \frac{b(\boldsymbol{\mu}; q, \boldsymbol{w})}{\|q\|_{Q^N} \|\boldsymbol{v}\|_{\boldsymbol{V}^N}} = \beta^N > 0.$$

in general the inf-sup is not guaranteed: approximation stability is needed.

Reduced Basis Method: approximation stability and spaces

How to fulfill the LBB inf-sup condition for the Reduced Basis case?

$$\inf_{q \in Q^N} \sup_{\boldsymbol{v} \in \boldsymbol{V}^N} \frac{b(\boldsymbol{\mu}; q, \boldsymbol{w})}{||q||_{Q^N} ||\boldsymbol{v}||_{\boldsymbol{V}^N}} = \beta^N > 0.$$

Some possibilities:

→ *supremizer enrichment* of the velocity space [Rozza and Veroy, 2007];

→ *Petrov-Galerkin projection* during online phase [Carlberg and Farhat, 2011], [Dahmen, 2014];

→ *Leray projection*

Reduced Basis Method: approximation stability and spaces

How to fulfill the LBB inf-sup condition for the Reduced Basis case?

$$\inf_{q \in Q^N} \sup_{\boldsymbol{v} \in \boldsymbol{V}^N} \frac{b(\boldsymbol{\mu}; q, \boldsymbol{w})}{\|q\|_{Q^N} \|\boldsymbol{v}\|_{\boldsymbol{V}^N}} = \beta^N > 0.$$

Some possibilities:

→ *supremizer enrichment* of the velocity space [Rozza and Veroy, 2007];
- \+ straightforward implementation;
- \+ standard finite dimensional Galerkin theory holds;
- \+ reliable, proven method [Ballarin et al., 2014];
- − larger RB spaces (and matrices);

→ *Petrov-Galerkin projection* during online phase [Carlberg and Farhat, 2011], [Dahmen, 2014];
- \+ simple online phase;
- − different sampling strategies for trial and test spaces;
- − very few results available;

→ *Leray projection*
- \+ no need to worry about compatibility conditions;
- \+ smaller RB spaces;
- − needs online pre-processing stage (mxm);
- − difficult implementation for complex geometries;

Leray projection

Helmholtz-Leray decomposition

Given a vector field $\boldsymbol{w}$, there is a unique decomposition: (see [Foias et al., 2001])

$$\boldsymbol{w} = \nabla\varphi + \boldsymbol{v} \quad \text{such that} \quad \operatorname{div} \boldsymbol{v} = 0$$

This can be seen as a special instance of the Piola transformation [Boffi et al., 2013]. Then, we define the *Leray projector* $\mathcal{P}_{\mathrm{L}} : \boldsymbol{w} \mapsto \boldsymbol{v}$. Applying $\mathcal{P}_{\mathrm{L}}$ to the reduced order formulation, the form $b(\boldsymbol{\mu}; q, \boldsymbol{v})$ is removed, and there is no need of the Q^N space.

Apply $\mathcal{P}_{\mathrm{L}}$ to each basis function $\overline{\zeta}_i$, in order to obtain a new, divergence-free basis $\{\overline{\zeta}^{\mathrm{div}}\}$.

The reduced basis solution will be in the form:

$$\boldsymbol{u}^N(\boldsymbol{\mu}) = \sum_{i=1}^{N} u_i^N(\boldsymbol{\mu})\overline{\boldsymbol{\zeta}}_i^{\mathrm{div}}$$

Leray projection

The snapshots are divergence free on the original domain:

$$\int_{\overline{\Omega}(\boldsymbol{\mu})} q \,\mathrm{div}\, \boldsymbol{u}(\boldsymbol{\mu}) \,\mathrm{d}\overline{\boldsymbol{x}} = 0 \qquad \forall q \in Q,$$

not on the reference domain, with a transformed divergence constraint:

$$\int_{\Omega} q \Big(\sum_{j=1}^{d} \sum_{k=1}^{d} G_{jk}(\mu, \boldsymbol{x}) \frac{\partial u^j(\boldsymbol{\mu})}{\partial x^k} \Big) J^{\mathrm{aff}}(\mu)^{-1} \,\mathrm{d}\boldsymbol{x} = 0.$$

To make them divergence-free on the reference domain, compute the projection:

$$\begin{cases} u_1^{\mathcal{N},\mathrm{div}} = \mathcal{P}_{\mathrm{L},1} \boldsymbol{u}^{\mathcal{N}} = G_{11}(\mu) u_1^{\mathcal{N}} + G_{12}(\mu) u_2^{\mathcal{N}} \\ u_2^{\mathcal{N},\mathrm{div}} = \mathcal{P}_{\mathrm{L},2} \boldsymbol{u}^{\mathcal{N}} = G_{21}(\mu) u_1^{\mathcal{N}} + G_{22}(\mu) u_2^{\mathcal{N}}. \end{cases}$$

Then, an orthonormal divergence-free basis $\{\zeta_i^{\mathrm{div}}\}$ on the reference domain is obtained applying the Gram-Schmidt orthogonalization method on the projected snapshots:

$$\boldsymbol{z}_i = \boldsymbol{u}^{\mathcal{N}}(\boldsymbol{\mu}^i) - \sum_{j=1}^{i-1} (\boldsymbol{u}^{\mathcal{N}}(\boldsymbol{\mu}^i), \boldsymbol{\zeta}_j)_0 \boldsymbol{\zeta}_j \qquad \boldsymbol{\zeta}_i = \frac{\boldsymbol{z}_i}{\|\boldsymbol{z}_i\|_0}.$$

Leray projection

What if we want to know pressure?

Two possibilities:

→ recover from the velocity coefficients:

$$p^N(\boldsymbol{\mu}) = \sum_{k=1}^{N} u_k^N(\boldsymbol{\mu})\sigma_k$$

→ solve a Poisson problem (online):

$$\Delta p^N(\boldsymbol{\mu}) = -\,\mathrm{div}\left(\boldsymbol{u}^N(\boldsymbol{\mu}) \cdot \nabla \boldsymbol{u}^N(\boldsymbol{\mu})\right)$$

Leray projection

The cooperation of the parametrized Leray projection $\mathcal{P}_{\mathrm{L}}(\mu)$ and the affine mapping $\mathcal{T}^{\mathrm{aff}}(\mu)$ can be visualized through the diagram:

$$\begin{tikzcd}
\boldsymbol{\zeta}_i \arrow[r, "\mathcal{T}(\mu)"] \arrow[d, "\mathcal{P}_{\mathrm{L}}(\overline{\mu})"'] & \overline{\boldsymbol{\zeta}}_i \arrow[d, "\mathcal{P}_{\mathrm{L}}(\mu)"] \\
\boldsymbol{\zeta}_i^{\mathrm{div}} \arrow[r, "\mathcal{P}_{\mathrm{L}}(\mu)\circ\mathcal{T}(\mu)"] & \overline{\boldsymbol{\zeta}}_i^{\mathrm{div}}
\end{tikzcd}$$

And the relationships between the spaces introduced this far are the following:

$$\begin{tikzcd}
\boldsymbol{V} \times Q \arrow[r, "\text{High Order}", "\text{Galerkin projection}"'] \arrow[d, "\mathcal{P}_{\mathrm{L}}"'] & \boldsymbol{V}^{\mathcal{N}} \times Q^{\mathcal{N}} \arrow[r, "\text{Reduced Basis}", "\text{Galerkin projection}"'] \arrow[d, "\mathcal{P}_{\mathrm{L}}"'] & \boldsymbol{V}^{N} \times Q^{N} \arrow[d, "\mathcal{P}_{\mathrm{L}}"] \\
\boldsymbol{V}_{\mathrm{div}} \arrow[r, "\text{High Order}", "\text{Galerkin projection}"'] & \boldsymbol{V}_{\mathrm{div}}^{\mathcal{N}} \arrow[r, "\text{Reduced Basis}", "\text{Galerkin projection}"'] & \boldsymbol{V}_{\mathrm{div}}^{N}
\end{tikzcd}$$

Reduced Basis Method: sampling technique

Centroidal Voronoi Tessellation

Given a distance function $\varrho : \mathcal{D} \to \mathbb{R}^+$ and a sequence of parameters $\{\boldsymbol{\mu}^i\}_{i=1}^{n-1}$, find the next element of the sequence $\boldsymbol{\mu}^n$ s. t.:

$$\sum_{i\in\tau_j} \varrho(\boldsymbol{\mu}^i)\|\boldsymbol{u}^{\mathcal{N}}(\boldsymbol{\mu}^i) - \boldsymbol{u}^{\mathcal{N}}(\boldsymbol{\mu}^n)\|_0^2 = \min_{\boldsymbol{\nu}\in\mathcal{D}} \sum_{i\in\tau_j} \varrho(\boldsymbol{\mu}^i)\|\boldsymbol{u}^{\mathcal{N}}(\boldsymbol{\mu}^i) - \boldsymbol{u}^{\mathcal{N}}(\boldsymbol{\nu})\|_0^2$$

with τ_j triangle in $\{\boldsymbol{\mu}^i\}_{i=1}^{n-1}$ with largest sum of $\varrho(\boldsymbol{\mu}^i)$. [Burkardt and Gunzburger, 2006]

As distance function, we choose

$$\varrho(\boldsymbol{\mu}^i) = \int_{\overline{\Omega}(\boldsymbol{\mu}^i)} \left[\boldsymbol{u}^{\mathcal{N}}(\boldsymbol{\mu}^i) - \mathcal{I}^N \boldsymbol{u}(\boldsymbol{\mu}^i)\right]^2 \mathrm{d}\overline{\boldsymbol{x}}$$

Two different CVTs, for steady state and time-dependent snapshots.

CVT gives hierarchical spaces (like POD and Greedy).

Alternatively: random sampling, Greedy (steady) [Prudhomme et al.,2003],[Rozza et al. 2008] and POD-Greedy (time-dependent) [Nguyen et al., 2009], [Haasdonk and Ohlberger, 2008]

Reduced Basis Method: sampling technique

Example of CVT sampling

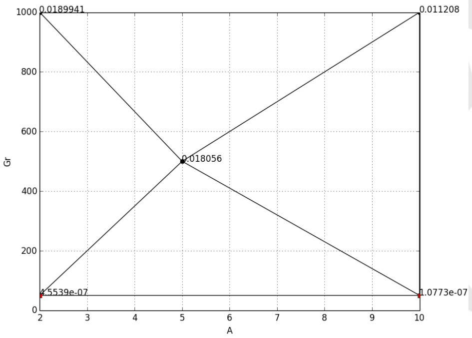

step 1

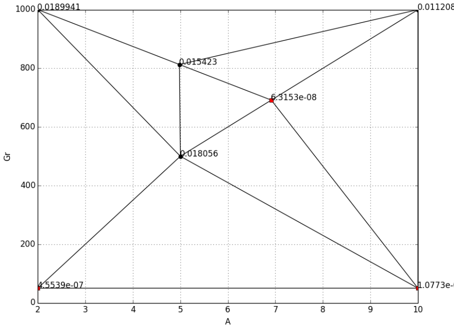

step 3

- → new point at barycenter of triangle with larger residuals;
- → weighted residual projection as error indicator;
- → special care needed for steady snapshots (if not, the CVT would sample only the high-Gr part of the parameter space $\mathcal{D}$).

Reduced Basis Method: sampling technique

Numerical example: a cavity flow with parametrized aspect ratio and Grashof number. This data refers to 55 offline runs, leading to 109 snapshots.

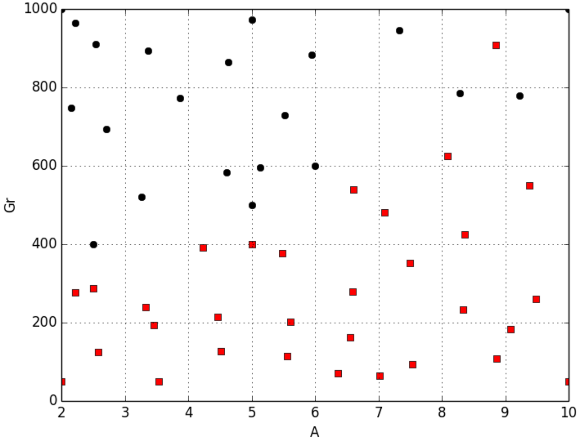

Parameters selected by the CVT sampling algorithm. With the red square mark we denote the steady state snapshots, with the black circle mark the time-dependent snapshots. The Grashof number is expressed in thousands.

Computational reduction of time-dependent snapshots

What to do with time-periodic snapshots? Proper Orthogonal Decomposition (POD). Given a series of snapshots $\boldsymbol{u}^{\mathcal{N}}(\boldsymbol{\mu}^i; \boldsymbol{x}, t^k)$ for $k = 1, N_{\mathrm{sn}}$, extract the more relevant information by finding the modes $\boldsymbol{\Psi}_i$ such that

$$\boldsymbol{\Psi}_i = \underset{\boldsymbol{\Psi}_1,\dots,\boldsymbol{\Psi}_{i-1}\in \boldsymbol{L}^2}{\arg\min} \ (\boldsymbol{v} - \sum_{j=1}^{i} (\boldsymbol{v}, \boldsymbol{\Psi}_j)_0 \boldsymbol{\Psi}_j) \quad \forall \boldsymbol{v} \in \boldsymbol{L}^2 \quad \text{such that} \quad (\boldsymbol{\Psi}_i, \boldsymbol{\Psi}_j)_0 = \delta_{ij}.$$

Practically, a possible algorithm is [Volkwein, Lecture notes]

i for each time-series, compute the *correlation matrix*

$$\mathbb{C}_{nm} = \int_{\overline{\Omega}(\boldsymbol{\mu})} \boldsymbol{u}^{\mathcal{N}}(\boldsymbol{\mu}^i; \boldsymbol{x}, t^n) \boldsymbol{u}^{\mathcal{N}}(\boldsymbol{\mu}^i; \boldsymbol{x}, t^m) \, \mathrm{d}\overline{\boldsymbol{x}}$$

ii compute the eigenpairs $(\lambda_k, \boldsymbol{\psi}_k)$ of $\mathbb{C}_{nm}$

iii compute the modes

$$\boldsymbol{\Psi}_k = \sum_{j=1}^{N_{\mathrm{sn}}} \psi_{k,j} \boldsymbol{u}^{\mathcal{N}}(\boldsymbol{\mu}^i; \boldsymbol{x}, t^j)$$

In this work, we keep the modes sufficient to store 99.9% of the energy (3 modes are sufficient for most cases).

The snapshots obtained with the POD are then passed to the orthogonalization procedure to build a reduced order basis.

Reduced Basis Method: Certification

Brezzi-Rappaz-Raviart theory. Main ingredients:

- continuity constant

$$\gamma^2(\boldsymbol{\mu}) = \sup_{w \in V} \sup_{z \in V} \sup_{v \in W} \frac{c(\boldsymbol{\mu}; \boldsymbol{w}, \boldsymbol{z}, \boldsymbol{v})}{\|\boldsymbol{w}\|_V \|\boldsymbol{z}\|_V \|\boldsymbol{v}\|_W}$$

- inf-sup constant

$$\beta_{\mathrm{LB}}^N \leq \beta^N \equiv \inf_{w \in V} \sup_{v \in W} \frac{D_u F_{\mathrm{NS}}(\boldsymbol{\mu}; \boldsymbol{w}, \boldsymbol{u}^N(\boldsymbol{\mu}), \boldsymbol{v})}{\|\boldsymbol{w}\|_V \|\boldsymbol{v}\|_W}$$

- dual norm of residual

$$\|r^N(\boldsymbol{\mu})\|_{V'} = \sup_{v \in W} \frac{F_{\mathrm{NS}}(\boldsymbol{\mu}; \boldsymbol{u}^N(\boldsymbol{\mu}), \boldsymbol{v})}{\|\boldsymbol{v}\|_W}$$

- adimensional residual measure

$$\tau^N(\boldsymbol{\mu}) \equiv \frac{4\gamma^2(\boldsymbol{\mu})}{(\beta_{\mathrm{LB}}^N)^2} \|r^N(\boldsymbol{\mu})\|_{V'}$$

Error estimate:

$$\|\boldsymbol{u}^{\mathcal{N}}(\boldsymbol{\mu}) - \boldsymbol{u}^N(\boldsymbol{\mu})\|_V \leq \Delta^N(\boldsymbol{\mu}) \equiv \frac{\beta_{\mathrm{LB}}^N}{2\gamma^2(\boldsymbol{\mu})} \left(1 - \sqrt{1 - \tau^N(\boldsymbol{\mu})}\right)$$

Reduced Basis Method: Certification

A posteriori error estimate

$$\|\boldsymbol{u}^{\mathcal{N}}(\boldsymbol{\mu}) - \boldsymbol{u}^{N}(\boldsymbol{\mu})\|_V \leq \Delta^N(\boldsymbol{\mu})$$

Works well for:

- $\longrightarrow$ steady Stokes, [Rozza et al., 2013];
- $\longrightarrow$ steady Navier-Stokes, sufficiently far from bifurcation points [Veroy and Patera, 2005], [Deparis 2008], [Manzoni, 2012];
- $\longrightarrow$ time-dependent Navier-Stokes, space-time framework [Urban and Patera, 2012], [Yano and Patera, 2013] main idea: Petrov-Galerkin projection on time-space functional settings e.g. $W \equiv L^2(I; \boldsymbol{H}_0^1) \times \boldsymbol{L}^2$.

Reduced Basis Method: Certification

For the bifurcation point: let $(\boldsymbol{\mu}_*, \boldsymbol{u}_*)$ simple bifurcation point, $(\boldsymbol{\mu}_*^N, \boldsymbol{u}_*^N)$ its approximation.

→ if branches intersect, let $(\boldsymbol{\mu}_i(s), \boldsymbol{u}_i(s)), i = 1, 2$ be their parametrization for each branch. We have:

$$|\boldsymbol{\mu}(s) - \boldsymbol{\mu}^N(s)| + \|\boldsymbol{u}(s) - \boldsymbol{u}^N(s)\|_X \leq C \inf_{v^N \in X^N} \|u(s) - v\|_X$$

→ if branches do not intesect (numerically), the distance between the solutions spaces is bounded:

$$d(\mathcal{S}^N, \mathcal{S}) \leq ch^{k-1/2};$$

If $(\boldsymbol{\mu}_0, \boldsymbol{u}_0)$ simple quadratic fold, [Brezzi et al., 1986], there are estimates of the type:

$$|\boldsymbol{\mu}_0^N(s) - \boldsymbol{\mu}_0| \leq c|s|^k.$$

BRANCHING PREDICTION

Steady bifurcations

Variational problem associated to the steady-state Navier-Stokes equations:

$$F_{\mathrm{S}}(\boldsymbol{\mu}; \boldsymbol{u}(\boldsymbol{\mu}), p(\boldsymbol{\mu})) = 0$$

with

$$F_{\mathrm{S}}(\boldsymbol{\mu}; \boldsymbol{u}(\boldsymbol{\mu}), p(\boldsymbol{\mu})) \begin{cases} c(\boldsymbol{\mu}; \boldsymbol{u}, \boldsymbol{u}, \boldsymbol{v}) + a(\boldsymbol{\mu}; \boldsymbol{u}, \boldsymbol{v}) + b(\boldsymbol{\mu}; \boldsymbol{v}, p) = \boldsymbol{f}(\boldsymbol{\mu}; \boldsymbol{v}) \\ b(\boldsymbol{\mu}; \boldsymbol{u}, q) \end{cases}$$

Tangent advection operator

Taking the Fréchet derivative of the convection term $\boldsymbol{u} \cdot \nabla \boldsymbol{u}$ about a steady solution $\boldsymbol{u}_0$, we have the linear operator $\boldsymbol{\mathcal{T}}(\boldsymbol{u}_0) : \boldsymbol{V} \to \boldsymbol{V}$:

$$\boldsymbol{\mathcal{T}}(\boldsymbol{u}_0)[\boldsymbol{v}] \equiv D_u F_S(\boldsymbol{u}_0)[\boldsymbol{v}] = \boldsymbol{u}_0 \cdot \nabla \boldsymbol{v} + \boldsymbol{v} \cdot \nabla \boldsymbol{u}_0. \tag{1}$$

If $\boldsymbol{u}_0(\boldsymbol{\mu}^*)$ is a bifurcation point, in a neighbourhood of $\boldsymbol{\mu}^* \in \mathcal{D}$ there is a change of sign for an eigenvalue σ_i of

$$T_{ij}(\boldsymbol{u}_0) = \boldsymbol{\mathcal{T}}((\boldsymbol{u}_0, \overline{\boldsymbol{\zeta}}_j^{\mathrm{div}})_0 \overline{\boldsymbol{\zeta}}_j^{\mathrm{div}})[\overline{\boldsymbol{\zeta}}_i^{\mathrm{div}}].$$

[Cliffe et al. 2012]

Numerical example: critical eigenvalue analysis

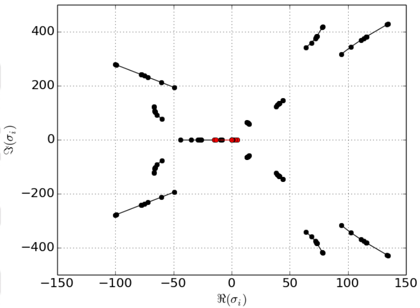

Eigenvalues of the operator $\mathcal{T}(u_0)$ in a neighbourhood of a steady bifurcation point.

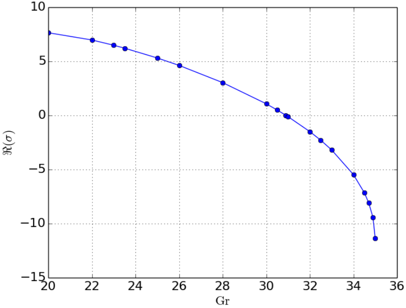

Real part of the critical eigenvalue of the operator $\mathcal{T}(u_0)$ in a neighbourhood of a steady bifurcation point.

Hopf bifurcation: unsteady solutions

Assuming a flow of period ω, formulate the time-dependent problem as

$$\omega \frac{\mathrm{d}\boldsymbol{u}}{\mathrm{d}t} = F_{\mathrm{S}}(\boldsymbol{\mu}; \boldsymbol{u}(\boldsymbol{\mu}), p(\boldsymbol{\mu}))$$

and we reconduce to the previous case [Ambrosetti and Prodi, 1992]:

$$F_{\mathrm{NS}}(\omega, \boldsymbol{\mu}; \boldsymbol{u}(\boldsymbol{\mu}), p(\boldsymbol{\mu})) = 0$$

where $F_{\mathrm{NS}} : \mathbb{R} \times \mathcal{D} \times \boldsymbol{V} \times Q \to \boldsymbol{V} \times Q$ is obtained from F_{S} by adding the time derivative.

Global linearized operator

Linearize the Navier-Stokes equations about a steady state $\boldsymbol{u}_0$ + small time perturbation $\boldsymbol{u}'(\boldsymbol{x})\mathrm{e}^{\sigma t}$:

$$\boldsymbol{\mathcal{L}}(\boldsymbol{u}_0)[\boldsymbol{u}'] = \boldsymbol{u}_0 \cdot \nabla \boldsymbol{u}' + \boldsymbol{u}' \cdot \nabla \boldsymbol{u}_0 - \Delta \boldsymbol{u}' = -\sigma \boldsymbol{u}'$$

$\to$ find eigenvalues of the operator $\boldsymbol{\mathcal{L}} : \boldsymbol{V} \to \boldsymbol{V}$:

$$\boldsymbol{\mathcal{L}}(\boldsymbol{u}_0)[\boldsymbol{u}'] = -\sigma \boldsymbol{u}'.$$

and if $\Re\sigma_0 > 0$, the perturbation will grow.

Hopf bifurcation

Global linearized operator

Linearize the Navier-Stokes equations about a steady state $\boldsymbol{u}_0$ + small time perturbation $\boldsymbol{u}'(\boldsymbol{x})\mathrm{e}^{\sigma t}$:

$$\boldsymbol{\mathcal{L}}(\boldsymbol{u}_0)[\boldsymbol{u}'] = \boldsymbol{u}_0 \cdot \nabla \boldsymbol{u}' + \boldsymbol{u}' \cdot \nabla \boldsymbol{u}_0 - \Delta \boldsymbol{u}' = -\sigma \boldsymbol{u}'$$

$\rightarrow$ find eigenvalues of the operator $\boldsymbol{\mathcal{L}} : \boldsymbol{V} \rightarrow \boldsymbol{V}$:

$$\boldsymbol{\mathcal{L}}(\boldsymbol{u}_0)[\boldsymbol{u}'] = -\sigma \boldsymbol{u}'.$$

and if $\Re\sigma_0 > 0$, the perturbation will grow.

In the reduced-basis context, find the eigenvalues of the matrix

$$L_{ij} = \sum_{k=1}^{N_{\boldsymbol{u}}} (\overline{\boldsymbol{\zeta}}_i^{\mathrm{div}}, \overline{\boldsymbol{\zeta}}_k^{\mathrm{div}} \cdot \nabla \overline{\boldsymbol{\zeta}}_j^{\mathrm{div}})_0 \, \boldsymbol{U}_N^k + \sum_{k=1}^{N_{\boldsymbol{u}}} (\overline{\boldsymbol{\zeta}}_i^{\mathrm{div}}, \overline{\boldsymbol{\zeta}}_j^{\mathrm{div}} \cdot \nabla \overline{\boldsymbol{\zeta}}_k^{\mathrm{div}})_0 \, \boldsymbol{U}_N^k + (\nabla \overline{\boldsymbol{\zeta}}_i^{\mathrm{div}}, \nabla \overline{\boldsymbol{\zeta}}_j^{\mathrm{div}})_0.$$

$L \in \mathbb{R}^{N \times N}$, and N is small, hence the eigenvalues can be computed with a good accuracy.

Time-dependent results

Frequencies at the onset of oscillatory solutions are determined by the imaginary part of the eigenvalues.

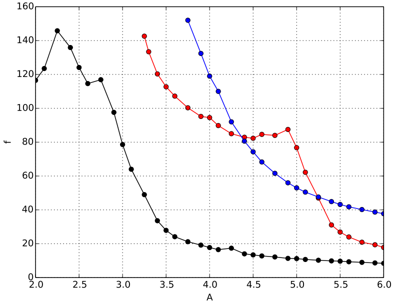

Frequences for the 1, 2 and 3-roll flows at the Hopf bifurcation.

- frequency qualitative behaviour follows expectations;
- some phase dispersion is present, better sampling might be needed near bifurcation values;

NUMERICAL RESULTS

Description of the benchmark problem

To validate the branching detection methods in a ROM context, we choose the GAMM benchmark on a buoyancy driven cavity flow [Roux, 1990].

The cavity has unitary height and parametrized length μ. In the limit of Prandtl $\to 0$, the forcing term is simply

$$\boldsymbol{f} = \mathrm{Gr}\, x \boldsymbol{\jmath}$$

with $\boldsymbol{\jmath}$ vertical versor, Gr the Grashof number. Velocity b. c. are homogeneous Dirichlet.

Hence, $\boldsymbol{\mu} = (\mathrm{Gr}\,, \mu)$, $\mathcal{D} = [50 \cdot 10^3, 1 \cdot 10^6] \times [2, 10]$, as used in the reference work of [Gelfgat et al., 1999].

Similar problem studied with POD and Reduced Basis by [Herrero et al., 2013]. Their approach: use different basis for each branch.

Some representative snapshots

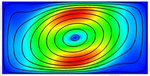

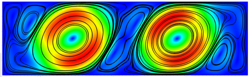

$\mu = 2, \mathrm{Gr} = 50$ S $\mu = 3.37, \mathrm{Gr} = 264.9$ U

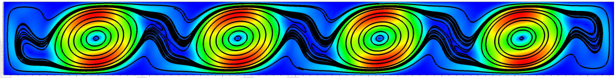

$\mu = 8.36, \mathrm{Gr} = 50.77$ S

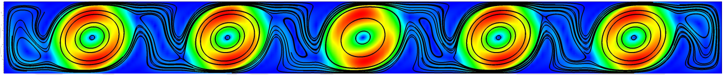

$\mu = 10, \mathrm{Gr} = 1$ U

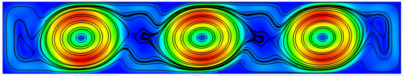

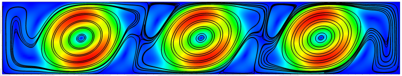

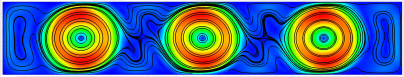

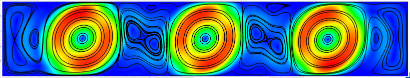

$\mu = 5.52, \mathrm{Gr} = 132.1$ U

Example: ROM for bifurcation diagram with $\mu = 4$

- → $N = 13$ (7 steady, 6 from POD with 99.9% energy threshold from two time-periodic snapshots);
- → reference works [Gelfgat et al., 1999] predict steady solutions with 1-roll, 2-roll and 3-roll flows;
- → continuation method during the offline phase;
- → computational time reduction: from 24-cpu hours on a cluster (PLX), to a few cpu-minutes per run on a personal PC.

Results agree with the reference results both in terms of the steady and the Hopf bifurcations; some hysteresis is shown also in the online phase.

CPU hours provided by CINECA (Consorzio Interuniversitario per l'Elaborazione ed il Calcolo Automatico) - ISCRA (Italian Super-Computing Resource Allocation) - project IsC13 - ID POOLSMR

Bifurcation diagram for $\mu = 4$

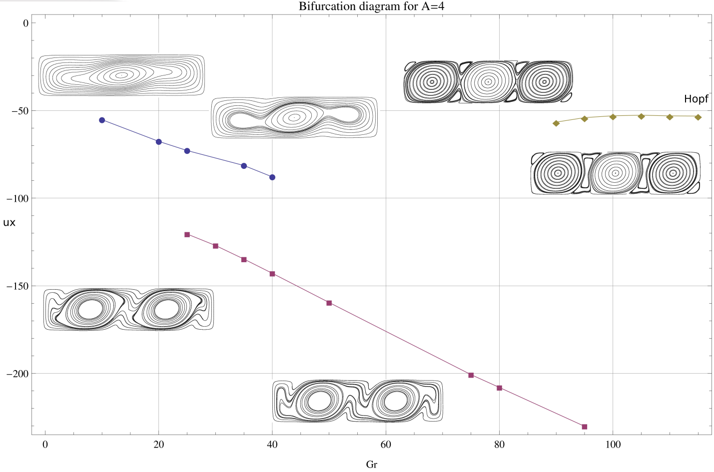

Bifurcation diagram for an aspect ratio of 4. The three lines are associated to the solutions with 1, 2, and 3 rolls. The horizontal velocity is taken at the point $(0.7, 0.7)$.

From [Pitton, Rozza, submitted, 2015]

Stability regions, reference: [Gelfgat et al., 1999]

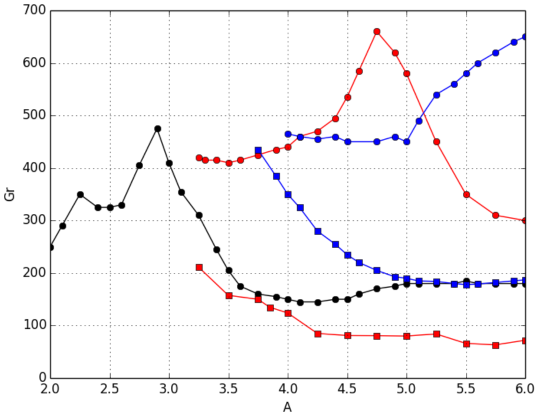

Stability regions for the 1-roll flows (in black), the 2-roll flows (red) and the 3-roll flows (blue). The Hopf bifurcation points are marked with the circles, the steady bifurcation points with the square marks. The Grashof number is expressed in thousands.

rough interpretation: 1-roll flows exist below the black line; 2-roll flows exist between the two red lines; 3-roll flows exist between the two blue lines.

Stability regions

We restrict ourselves to the region $(\mu, \mathrm{Gr}) \in [50 \cdot 10^3, 1 \cdot 10^6] \times [2, 6]$.

This time $N = 108$, but each simulation is run with a lower number of basis functions, depending on the parameter zone of interest.

Hopf bifurcations are detected by using a set of basis (deriving from snapshots) with an equal number of rolls.

Steady bifurcations are detected by using basis with an equal number of rolls, plus some different basis close to the parameter range.

Computational gain: reduced order computing time is $\simeq 0.35\%$ of the full order (5 minutes on a personal computer vs 24 cpu-hours on a cluster).

Time-dependent results

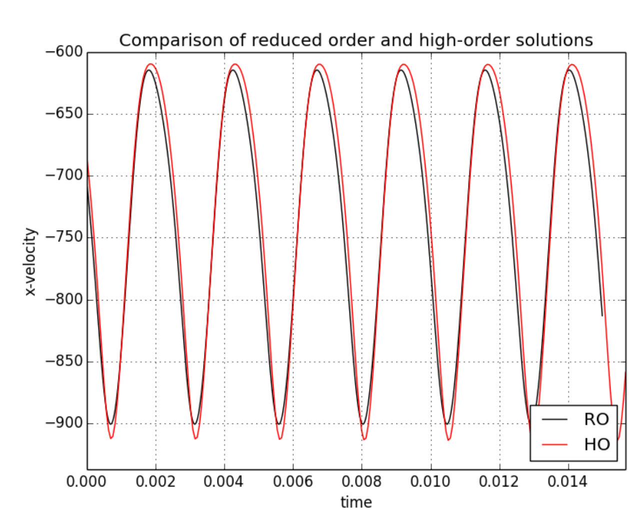

Comparison of the horizontal velocity at a the point $(0.7, 0.7)$ vs time for the high order (in red) and reduced order (in black) simulations. The parameters are $\mathrm{Gr} = 963791$, $A = 2.22$, and the resulting flow has a single roll.

Time-dependent results

High-Order solution

Reduced-Order solution

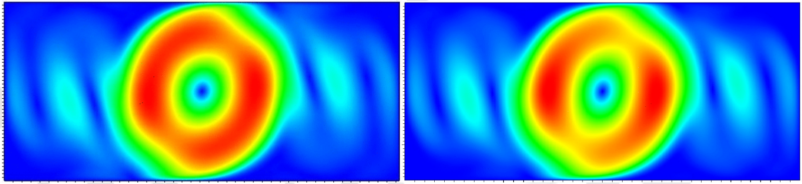

2D sudden expansion channel

Onset of Coanda effect in mitral valves (benchmark from [Drikakis, 1996])

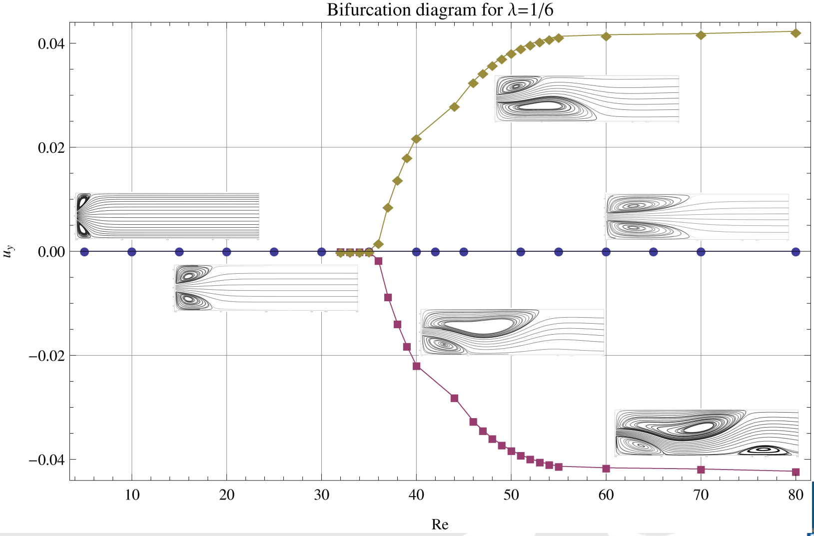

Symmetry breaking bifurcation for a channel with orifice. Vertical velocity is taken at the mean horizontal line, at distance 1 from the inlet.

2D variable geometry

First step: 2D parametrization

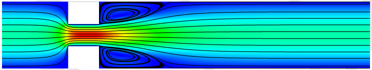

$A = 1/3, \ \mathrm{Re} = 45$

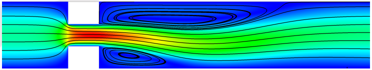

$A = 1/3, \ \mathrm{Re} = 100$

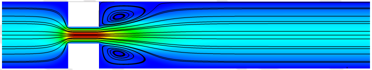

$A = 1/4, \ \mathrm{Re} = 30$

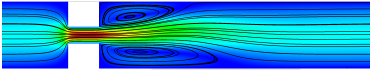

$A = 1/4, \ \mathrm{Re} = 50$

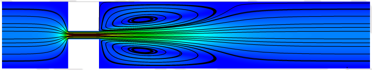

$A = 1/8, \ \mathrm{Re} = 40$

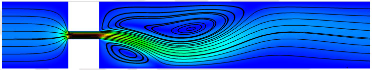

$A = 1/8, \ \mathrm{Re} = 40$

3D sudden expansion channel

Second step: reference 3D simplified geometry (benchmark from [Oliveira et al., 2008])

Re = 7.8

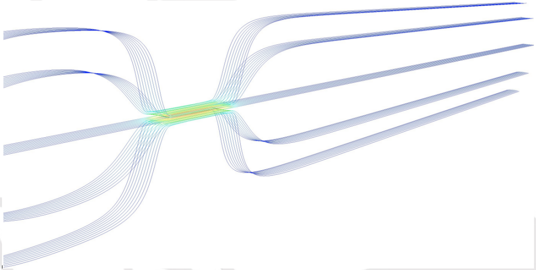

Re = 100

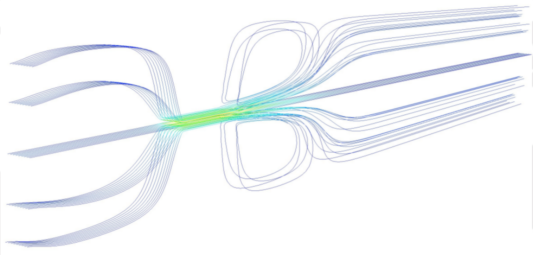

3D sudden expansion channel

Second step: reference 3D simplified geometry (benchmark from [Oliveira et al., 2008])

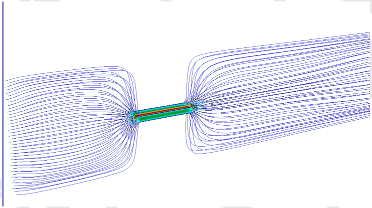

Re $= 7.3$

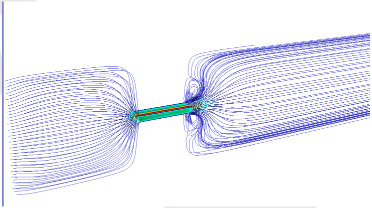

Re $= 18.2$

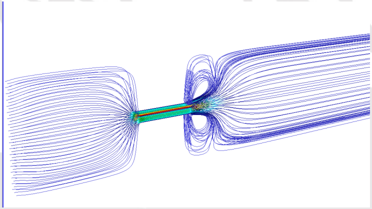

Re $= 25.5$

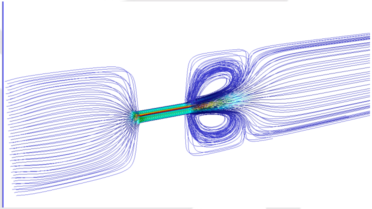

Re $= 43.7$

Perspectives

- → goal: investigate the possibility of using ROM techniques for bifurcation problems in Fluid Dynamics (first results are encouraging);
- → application: provide computational reduction tools for Coanda effect in haemodynamics applications;
- → combine precision of high order schemes (e.g. SEM) with low cost of Reduced Basis methods;
- → future investigation areas (with University of Houston):
  - → geometrical parametrization;
  - → 2D/3D effects;
  - → more complex model/tests with elastic wall/valve (FSI).

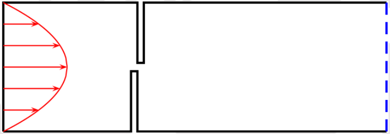

Scheme of prolapse geometry

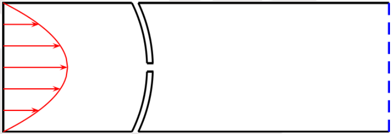

Scheme of elastic valve

Collaborations & Sponsors

Collaborations in ROM framework (2003-2015)

A. Quarteroni	A. T. Patera	Y. Maday	P. Huynh
K. Veroy	T. Lassila	F. Ballarin	J. Hesthaven
A. Manzoni	P. Chen	L. Iapichino	B. Stamm
F. Negri	D. Devaud	D. Forti	K. Urban
P. Pacciarini	G. Pitton	F. Salmoiraghi	A. Sartori
A. Quaini	L. Heltai	C. Nguyen	S. Deparis
I. Maier	B. Haasdonk	S. Volkwein	A. De Simone
M. Grepl	M. Ohlberger	L. Dedè	

Sponsors

SISSA NOFYSAS Excellence Grant, PRIN 2012 MIUR, European Cooperation in Science and Technology COST: EU-MORNET TD1307, Swiss National Science Foundation, INdAM-GNCS, Regione Friuli Venezia Giulia, DITENAVE, Danieli RC, European Research Council - Mathcard Project, MIT-Italy Program, Area Science Park Innovation Network.

SISSA mathLab

- A new center for mathematical modelling and numerical simulation at SISSA: mathLab
- A new PhD program: Mathematical Analysis, Modelling and Applications
- A new master in High Performance Computing
- A new supercomputing center in Miramare: Ulysses cluster (100TFlops)

Faculties: 3, Research Staff: 8, PhD+grad+postgrad: 8

Director: A. De Simone, Head Scientific Com.: A. Quarteroni

ma per seguir virtute e canoscenza SISSA

sissa mathLab innovating with mathematics

MHPC Master in High Performance Computing

SISSA **WORKSHOP**

MoRePaS 2015

Model Reduction of Parametrized Systems III

WHEN

OCTOBER 13th TO 16th, 2015

WHERE

SISSA
Via Bonomea, 265
Trieste - Italy

MORE INFO

http://www.sissa.it/morepas2015

CONTACTS

morepas2015@sissa.it

DEADLINES

Contributed Abstracts Submission: **July 1**
Abstracts Acceptance Notification: **July 20**
Early Registration: **August 15**
Late Registration: **September 15**

TOPICS

- Reduced basis methods
- Proper orthogonal decomposition
- Proper generalized decomposition
- Approximation theory related to model reduction
- Learning theory and compressed sensing
- Stochastic and high-dimensional problems
- System-theoretic methods
- Nonlinear Model Reduction
- Reduction of coupled problems/ multiphysics
- Optimization and optimal control
- State estimation and control
- Reduced order models and domain decomposition methods
- Krylov-subspace and interpolatory methods
- Application to real, industrial and complex problems

EXECUTIVE/SCIENTIFIC COMMITTEE

Gianluigi Rozza (SISSA, Trieste, Italy), *Chair*
Karsten Urban (Ulm University, Germany), *co-Chair*
Peter Benner (MPI Magdeburg, Germany)
Mario Ohlberger (University of Münster, Germany)
Danny Sorensen (Rice University, USA)

Anthony Patera (MIT, Cambride, USA)
Scientific Committee coordinator
Charbel Farhat (Stanford University, USA)
Martin Grepl (RWTH Aachen, Germany)
Serkan Gugercin (Virginia Tech, USA)
Bernard Haasdonk (University of Stuttgart, Germany)
Tony Lelievre (ENPC ParisTech, France)
Yvon Maday (Paris VI, France)
Wil Schilders (TU Eindhoven, Netherlands)
Danny Sorensen (Rice University, USA)
Karen Veroy-Grepl (RWTH Aachen, Germany)
Stefan Volkwein (University of Konstanz, Germany)
Karen Willcox (MIT, Cambridge, USA)

LOCAL ORGANIZING COMMITTEE

SISSA mathLab team

SPEAKERS

David Amsallem, Stanford University (US)
Thanos Antoulas, Rice University (US)
Tobias Breiten, Universität Graz (Austria)
Christopher Beattie, Virginia Tech (US)
Matthias Heinkenschloss, Rice University (US)
Sameer Kher, ANSYS (US)
Gitta Kutyniok, Technische Universität Berlin (Germany)
Anthony Nouy, Ecole Centrale de Nantes (France)
Simona Perotto, Politecnico di Milano (Italy)
Christoph Schwab, ETH Zürich (Switzerland)
Masayuki Yano, MIT (US)

The event is supported and organized in the framework of COST (European Cooperation in Science and Technology) initiative EU-MORNET: European Union Model Reduction Network (TD1307).

MoRePaS 2015 EU-MORNET European Network for Model Reduction cost sissa mathLab innovating with mathematics SISSA

SISSA **WORKSHOP**

MoRePaS 2015

Model Reduction of Parametrized Systems III

WHEN

OCTOBER 13th TO 16th, 2015

WHERE

SISSA
Via Bonomea, 265
Trieste - Italy

MORE INFO

http://www.sissa.it/morepas2015

CONTACTS

morepas2015@sissa.it

DEADLINES

Contributed Abstracts
Submission: **July 1**
Abstracts Acceptance
Notification: **July 20**
Early Registration: **August 15**
Late Registration: **September 15**

TOPICS

- Reduced basis methods
- Proper orthogonal decomposition
- Proper generalized decomposition
- Approximation theory related to model reduction
- Learning theory and compressed sensing
- Stochastic and high-dimensional problems
- System-theoretic methods
- Nonlinear Model Reduction
- Reduction of coupled problems/multiphysics
- Optimization and optimal control
- State estimation and control
- Reduced order models and domain decomposition methods
- Krylov-subspace and interpolatory methods
- Application to real, industrial and complex problems

EXECUTIVE/SCIENTIFIC COMMITTEE

Gianluigi Rozza (SISSA, Trieste, Italy), *Chair*
Karsten Urban (Ulm University, Germany), *co-Chair*
Peter Benner (MPI Magdeburg, Germany)
Mario Ohlberger (University of Münster, Germany)
Danny Sorensen (Rice University, USA)

Anthony Patera (MIT, Cambride, USA)
Scientific Committee coordinator
Charbel Farhat (Stanford University, USA)
Martin Grepl (RWTH Aachen, Germany)
Serkan Gugercin (Virginia Tech, USA)
Bernard Haasdonk (University of Stuttgart, Germany)
Tony Lelievre (ENPC ParisTech, France)
Yvon Maday (Paris VI, France)
Wil Schilders (TU Eindhoven, Netherlands)
Danny Sorensen (Rice University, USA)
Karen Veroy-Grepl (RWTH Aachen, Germany)
Stefan Volkwein (University of Konstanz, Germany)
Karen Willcox (MIT, Cambridge, USA)

LOCAL ORGANIZING COMMITTEE

SISSA mathLab team

The event is supported and organized in the framework of COST (European Cooperation in Science and Technology) initiative EU-MORNET: European Union Model Reduction Network (TD1307).


Thank You

References

A. Ambrosetti, G. Prodi
A Primer of Nonlinear Analysis
Cambridge University Press, 1995

M. Barrault, Y. Maday, N. C. Nguyen, A. T. Patera
An 'empirical interpolation' method: application to efficient reduced-basis discretization of partial differential equations
C. R. Acad. Sci. Paris, Ser. I, 2004

F. Brezzi,
Finite dimensional approximation of nonlinear problems
Numerische Mathematik, 1981

F. Brezzi, M. Cornalba, A. Di Carlo
How to get around a simple quadratic fold
Numerische Mathematik, 1986

D. Boffi, F. Brezzi, M. Fortin
Mixed Finite Element Methods and Applications
Springer, 2013

References

J. Burkardt, M. Gunzburger, H.-C. Lee
POD and CVT-based reduced-order modeling of Navier-Stokes flows
Comp. Meth. Appl. Mech. Engrg., 2006

K. A. Cliffe, E. J.C. Hall, P. Houston, E. T. Phipps, A. G. Salinger
Adaptivity and a Posteriori Error Control for Bifurcation Problems III: Incompressible Fluid Flow in Open Systems with O(2) Symmetry
Journal of Scientific Computing, 2012

S. Deparis
Reduced basis error bound computation of parameter-dependent Navier-Stokes equations by the natural norm approach
SIAM Journal on Numerical Analysis, 2008

D. Drikakis
Bifurcation phenomena in incompressible sudden expansion flows
Phys. Fluids, 1997

References

C. Foias, O. Manley, R. Rosa, R. Temam
Navier-Stokes Equations and Turbulence
Cambridge University Press, 2001

A. Y. Gelfgat, P. Z. Bar-Yoseph, A. L. Yarin
Stability of multiple steady states of convection in laterally heated cavities
Journal of Fluid Mechanics, 1999

B. Haasdonk, M. Ohlberger
Reduced Basis Method for Finite Volume Approximations of Parametrized Linear Evolution Equations
Math. Model. Numer. Anal., 2008

H. Herrero, Y. Maday, F. Pla
RB (Reduced Basis) for RB (Rayleigh-Bénard)
Comp. Methods Appl. Mech. Eng., 2013

References

D. J. Knezevic, N. C. Nguyen, A. T. Patera
Reduced Basis Approximation and A Posteriori Error Estimation for the Parametrized Unsteady Boussinesq Equations
Math. Models Methods Appl. Sci., 2010

N. C. Nguyen, G. Rozza, A. T. Patera
Reduced Basis Approximation and A Posteriori Error Estimation for the Time-Dependent Viscous Burgers Equation
Calcolo, 2009

A. K. Noor, C. M. Andersen, J. M. Peters
Reduced Basis Technique for Collapse Analysis of Shells
AIAA Journal, 1981

M. S. N. Oliveira, L. E. Rodd, G. H. McKinley, M. A. Alves
Simulations of extensional flows in microrheometric devices
Microfluid Nanofluid, 2008

References

J. S. Peterson
The Reduced Basis Method for Incompressible Viscous Flow Calculations
SIAM J. Sci. Stat. Comp, 1989

B. Roux, ed.
Numerical Simulation of Oscillatory Convection in Low-Pr Fluids
Springer, 1990

G. Rozza, D.B.P. Huynh, A. Manzoni
Reduced basis approximation and a posteriori error estimation for Stokes flows in parametrized geometries: roles of the inf-sup stability constants
Numerische Mathematik, 2013

G. Rozza, D.B.P. Huynh, A. T. Patera
Reduced Basis Approximation and a Posteriori Error Estimation for Affinely Parametrized Elliptic Coercive Partial Differential Equations
Arch. Comp. Methods Eng., 2008

References

G. Rozza, K. Veroy
On the stability of the reduced basis method for Stokes equations on parametrized domains
Comp. Methods Appl. Mech. Eng., 2007

I. J. Sobey, P. G. Drazin
Bifurcations of two-dimensional channel flows
J. Fluid Mech., 1986

A. G. Tomboulides, J. C. Y. Lee, S. A. Orszag
Numerical Simulation of Low Mach Number Reactive Flows
Journal of Scientific Computing, 1997

K. Urban, A. T. Patera
A new error bound for reduced basis approximation of parabolic partial differential equations
C. R. Acad. Sci. Paris Ser. I, 2012

References

- K. Veroy and A.T. Patera
  Certified real-time solution of the parametrized steady incompressible Navier-Stokes equations: Rigorous reduced-basis a posteriori error bounds
  Internat. J. Numer. Methods Fluids, 2005
- K. Veroy, C. Prud'Homme, D.V. Rovas, A. Patera
  A Posteriori Error Bounds for Reduced-Basis Approximation of Parametrized Noncoercive and Nonlinear Elliptic Partial Differential Equations
  AIAA Paper 2003-3847, 2003
- S. Volkwein
  Proper Orthogonal Decomposition: Theory and Reduced-Order Modelling
  Lecture notes, 2013
- M. Yano, A. T. Patera
  A space-time variational approach to hydrodynamic stability theory
  Proc. R. Soc. Ser. A, 2013